LETTERS

Two-dimensional gas of massless Dirac fermions in graphene

K. S. Novoselov[1], A. K. Geim[1], S. V. Morozov[2], D. Jiang[1], M. I. Katsnelson[3], I. V. Grigorieva[1], S. V. Dubonos[2] & A. A. Firsov[2]

Quantum electrodynamics (resulting from the merger of quantum mechanics and relativity theory) has provided a clear understanding of phenomena ranging from particle physics to cosmology and from astrophysics to quantum chemistry[1–3]. The ideas underlying quantum electrodynamics also influence the theory of condensed matter[4,5], but quantum relativistic effects are usually minute in the known experimental systems that can be described accurately by the non-relativistic Schrödinger equation. Here we report an experimental study of a condensed-matter system (graphene, a single atomic layer of carbon[6,7]) in which electron transport is essentially governed by Dirac's (relativistic) equation. The charge carriers in graphene mimic relativistic particles with zero rest mass and have an effective 'speed of light' $c_* \approx 10^6$ m s^{-1}. Our study reveals a variety of unusual phenomena that are characteristic of two-dimensional Dirac fermions. In particular we have observed the following: first, graphene's conductivity never falls below a minimum value corresponding to the quantum unit of conductance, even when concentrations of charge carriers tend to zero; second, the integer quantum Hall effect in graphene is anomalous in that it occurs at half-integer filling factors; and third, the cyclotron mass m_c of massless carriers in graphene is described by $E = m_c c_*^2$. This two-dimensional system is not only interesting in itself but also allows access to the subtle and rich physics of quantum electrodynamics in a bench-top experiment.

Graphene is a monolayer of carbon atoms packed into a dense honeycomb crystal structure that can be viewed as an individual atomic plane extracted from graphite, as unrolled single-wall carbon nanotubes or as a giant flat fullerene molecule. This material has not been studied experimentally before and, until recently[6,7], was presumed not to exist in the free state. To obtain graphene samples we used the original procedures described in ref. 6, which involve the micromechanical cleavage of graphite followed by the identification and selection of monolayers by using a combination of optical microscopy, scanning electron microscopy and atomic-force microscopy. The selected graphene films were further processed into multi-terminal devices such as that shown in Fig. 1, by following standard microfabrication procedures[7]. Despite being only one atom thick and unprotected from the environment, our graphene devices remain stable under ambient conditions and exhibit high mobility of charge carriers. Below we focus on the physics of 'ideal' (single-layer) grapheme, which has a different electronic structure and exhibits properties qualitatively different from those characteristic of either ultrathin graphite films (which are semimetals whose material properties were studied recently[7–10]) or even of other devices consisting of just two layers of graphene (see below).

Figure 1 shows the electric field effect[7–9] in graphene. Its conductivity σ increases linearly with increasing gate voltage V_g for both polarities, and the Hall effect changes its sign at $V_g \approx 0$. This behaviour shows that substantial concentrations of electrons (holes) are induced by positive (negative) gate voltages. Away from the transition region $V_g \approx 0$, Hall coefficient $R_H = 1/ne$ varies as $1/V_g$, where n is the concentration of electrons or holes and e is the electron charge. The linear dependence $1/R_H \propto V_g$ yields $n = \alpha V_g$ with $\alpha \approx 7.3 \times 10^{10}$ cm^{-2} V^{-1}, in agreement with the theoretical estimate $n/V_g \approx 7.2 \times 10^{10}$ cm^{-2} V^{-1} for the surface charge density induced by the field effect (see the caption to Fig. 1). The agreement indicates that all the induced carriers are mobile and that there are no trapped charges in graphene. From the linear dependence $\sigma(V_g)$ we found carrier mobilities $\mu = \sigma/ne$, which reached 15,000 cm^2 V^{-1} s^{-1} for both electrons and holes, were independent of temperature T between 10 and 100 K and were probably still limited by defects in parent graphite.

To characterize graphene further, we studied Shubnikov-de Haas oscillations (SdHOs). Figure 2 shows examples of these oscillations for different magnetic fields B, gate voltages and temperatures. Unlike ultrathin graphite[7], graphene exhibits only one set of SdHO for both electrons and holes. By using standard fan diagrams[7,8] we have determined the fundamental SdHO frequency B_F for various V_g. The resulting dependence of B_F on n is plotted in Fig. 3a. Both carriers exhibit the same linear dependence $B_F = \beta n$, with $\beta \approx 1.04 \times 10^{-15}$ Tm^2 ($\pm 2\%$). Theoretically, for any two-dimensional (2D) system β is defined only by its degeneracy f so that $B_F = \phi_0 n/f$, where $\phi_0 = 4.14 \times 10^{-15}$ Tm^2 is the flux quantum. Comparison with the experiment yields $f = 4$, in agreement with the double-spin and double-valley degeneracy expected for graphene[11,12] (see caption to Fig. 2). Note, however, an anomalous feature of SdHO in graphene, which is their phase. In contrast to conventional metals, graphene's longitudinal resistance $\rho_{xx}(B)$ exhibits maxima rather than minima at integer values of the Landau filling factor ν (Fig. 2a). Figure 3b emphasizes this fact by comparing the phase of SdHO in graphene with that in a thin graphite film[7]. The origin of the 'odd' phase is explained below.

Another unusual feature of 2D transport in graphene clearly reveals itself in the dependence of SdHO on T (Fig. 2b). Indeed, with increasing T the oscillations at high V_g (high n) decay more rapidly. One can see that the last oscillation ($V_g \approx 100$ V) becomes practically invisible at 80 K, whereas the first one ($V_g < 10$V) clearly survives at 140 K and remains notable even at room temperature. To quantify this behaviour we measured the T-dependence of SdHO's amplitude at various gate voltages and magnetic fields. The results could be fitted accurately (Fig. 3c) by the standard expression $T/\sinh(2\pi^2 k_B T m_c/\hbar e B)$, which yielded m_c varying between $\sim$0.02 and $0.07 m_0$ (m_0 is the free electron mass). Changes in m_c are well described by a square-root dependence $m_c \propto n^{1/2}$ (Fig. 3d).

To explain the observed behaviour of m_c, we refer to the semiclassical expressions $B_F = (\hbar/2\pi e)S(E)$ and $m_c = (\hbar^2/2\pi)\partial S(E)/\partial E$,

[1]Manchester Centre for Mesoscience and Nanotechnology, University of Manchester, Manchester M13 9PL, UK. [2]Institute for Microelectronics Technology, 142432 Chernogolovka, Russia. [3]Institute for Molecules and Materials, Radboud University of Nijmegen, Toernooiveld 1, 6525 ED Nijmegen, The Netherlands.

where $S(E) = \pi k^2$ is the area in k-space of the orbits at the Fermi energy $E(k)$ (ref. 13). If these expressions are combined with the experimentally found dependences $m_c \propto n^{1/2}$ and $B_F = (h/4e)n$ it is straightforward to show that S must be proportional to E^2, which yields $E \propto k$. The data in Fig. 3 therefore unambiguously prove the linear dispersion $E = \hbar k c_*$ for both electrons and holes with a common origin at $E = 0$ (refs 11, 12). Furthermore, the above equations also imply $m_c = E/c_*^2 = (h^2 n/4\pi c_*^2)^{1/2}$ and the best fit to our data yields $c_* \approx 10^6\,\mathrm{m\,s^{-1}}$, in agreement with band structure calculations[11,12]. The semiclassical model employed is fully justified by a recent theory for graphene[14], which shows that SdHO's amplitude can indeed be described by the above expression $T/\sinh(2\pi^2 k_B T m_c/\hbar e B)$ with $m_c = E/c_*^2$. Therefore, even though the linear spectrum of fermions in graphene (Fig. 3e) implies zero rest mass, their cyclotron mass is not zero.

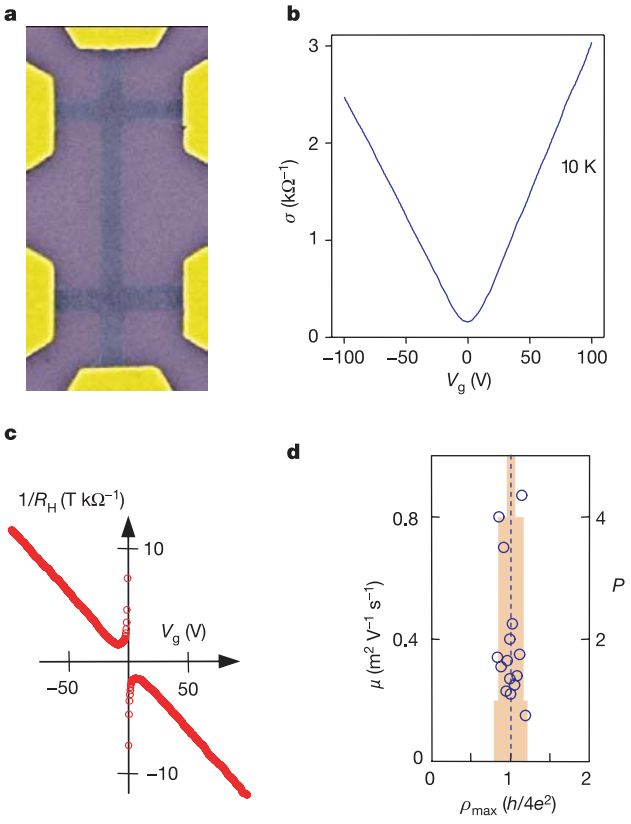

Figure 1 | Electric field effect in graphene. **a**, Scanning electron microscope image of one of our experimental devices (the width of the central wire is 0.2 μm). False colours are chosen to match real colours as seen in an optical microscope for large areas of the same material. **b**, **c**, Changes in graphene's conductivity σ (**b**) and Hall coefficient R_H (**c**) as a function of gate voltage V_g. σ and R_H were measured in magnetic fields B of 0 and 2 T, respectively. The induced carrier concentrations n are described in ref. 7; $n/V_g = \varepsilon_0\varepsilon/te$, where ε_0 and ε are the permittivities of free space and SiO_2, respectively, and $t \approx 300$ nm is the thickness of SiO_2 on top of the Si wafer used as a substrate. $R_H = 1/ne$ is inverted to emphasize the linear dependence $n \propto V_g$. $1/R_H$ diverges at small n because the Hall effect changes its sign at about $V_g = 0$, indicating a transition between electrons and holes. Note that the transition region ($R_H \approx 0$) was often shifted from zero V_g as a result of chemical doping[7], but annealing of our devices in vacuum normally allowed us to eliminate the shift. The extrapolation of the linear slopes $\sigma(V_g)$ for electrons and holes results in their intersection at a value of σ indistinguishable from zero. **d**, Maximum values of resistivity $\rho = 1/\sigma$ (circles) exhibited by devices with different mobilities μ (left y axis). The histogram (orange background) shows the number P of devices exhibiting ρ_{max} within 10% intervals around the average value of $\sim h/4e^2$. Several of the devices shown were made from two or three layers of graphene, indicating that the quantized minimum conductivity is a robust effect and does not require 'ideal' graphene.

The unusual response of massless fermions to a magnetic field is highlighted further by their behaviour in the high-field limit, at which SdHOs evolve into the quantum Hall effect (QHE). Figure 4 shows the Hall conductivity σ_{xy} of graphene plotted as a function of electron and hole concentrations in a constant B. Pronounced QHE plateaux are visible, but they do not occur in the expected sequence $\sigma_{xy} = (4e^2/h)N$, where N is integer. On the contrary, the plateaux correspond to half-integer ν so that the first plateau occurs at $2e^2/h$ and the sequence is $(4e^2/h)(N + 1/2)$. The transition from the lowest hole ($\nu = -1/2$) to the lowest electron ($\nu = +1/2$) Landau level (LL) in graphene requires the same number of carriers ($\Delta n = 4B/\phi_0 \approx 1.2 \times 10^{12}\,\mathrm{cm^{-2}}$) as the transition between other nearest levels (compare the distances between minima in ρ_{xx}). This results in a ladder of equidistant steps in σ_{xy} that are not interrupted when passing through zero. To emphasize this highly unusual behaviour, Fig. 4 also shows σ_{xy} for a graphite film consisting of only two graphene layers, in which the sequence of plateaux returns to normal and the first plateau is at $4e^2/h$, as in the conventional QHE. We attribute this qualitative transition between graphene and its two-layer counterpart to the fact that fermions in the latter exhibit a finite mass near $n \approx 0$ and can no longer be described as massless Dirac particles.

The half-integer QHE in graphene has recently been suggested by two theory groups[15,16], stimulated by our work on thin graphite films[7] but unaware of the present experiment. The effect is single-particle and is intimately related to subtle properties of massless Dirac fermions, in particular to the existence of both electron-like and hole-like Landau states at exactly zero energy[14–17]. The latter can be viewed as a direct consequence of the Atiyah–Singer index theorem that is important in quantum field theory and the theory of superstrings[18,19]. For 2D massless Dirac fermions, the theorem guarantees the existence of Landau states at $E = 0$ by relating the difference in the number of such states with opposite chiralities to the total flux through the system (magnetic field can be inhomogeneous).

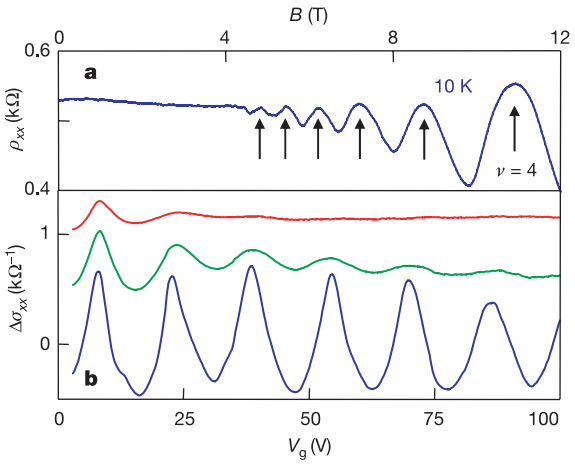

Figure 2 | Quantum oscillations in graphene. SdHO at constant gate voltage $V_g = -60$ V as a function of magnetic field B (**a**) and at constant $B = 12$ T as a function of V_g (**b**). Because μ does not change greatly with V_g, the measurements at constant B (at a constant $\omega_c\tau = \mu B$) were found more informative. In **b**, SdHOs in graphene are more sensitive to T at high carrier concentrations: blue, $T = 20$ K; green, $T = 80$ K; red, $T = 140$ K. The $\Delta\sigma_{xx}$ curves were obtained by subtracting a smooth (nearly linear) increase in σ with increasing V_g and are shifted for clarity. SdHO periodicity ΔV_g at constant B is determined by the density of states at each Landau level ($\alpha\Delta V_g = fB/\phi_0$), which for the observed periodicity of ~15.8 V at $B = 12$ T yields a quadruple degeneracy. Arrows in **a** indicate integer ν (for example, $\nu = 4$ corresponds to 10.9 T) as found from SdHO frequency $B_F \approx 43.5$ T. Note the absence of any significant contribution of universal conductance fluctuations (see also Fig. 1) and weak localization magnetoresistance, which are normally intrinsic for 2D materials with so high resistivity.

To explain the half-integer QHE qualitatively, we invoke the formal expression[2,14–17] for the energy of massless relativistic fermions in quantized fields, $E_N = [2e\hbar c_*^2 B(N + 1/2 \pm 1/2)]^{1/2}$. In quantum electrodynamics, the sign $\pm$ describes two spins, whereas in graphene it refers to 'pseudospins'. The latter have nothing to do with the real spin but are 'built in' to the Dirac-like spectrum of graphene; their origin can be traced to the presence of two carbon sublattices. The above formula shows that the lowest LL ($N = 0$) appears at $E = 0$ (in agreement with the index theorem) and accommodates fermions with only one (minus) projection of the pseudospin. All other levels $N \geq 1$ are occupied by fermions with both ($\pm$) pseudospins. This implies that for $N = 0$ the degeneracy is half of that for any other N. Alternatively, one can say that all LLs have the same 'compound' degeneracy but the zero-energy LL is shared equally by electrons and holes. As a result the first Hall plateau occurs at half the normal filling and, oddly, both $\nu = -1/2$ and $+1/2$ correspond to the same LL ($N = 0$). All other levels have normal degeneracy $4B/\phi_0$ and therefore remain shifted by the same 1/2 from the standard sequence. This explains the QHE at $\nu = N + 1/2$ and, at the same time, the 'odd' phase of SdHO (minima in ρ_{xx} correspond to plateaux in ρ_{xy} and therefore occur at half-integer ν; see Figs 2 and 4), in agreement with theory[14–17]. Note, however, that from another perspective the phase shift can be viewed as the direct manifestation of Berry's phase acquired by Dirac fermions moving in magnetic field[20,21].

Finally, we return to zero-field behaviour and discuss another feature related to graphene's relativistic-like spectrum. The spectrum implies vanishing concentrations of both carriers near the Dirac point $E = 0$ (Fig. 3e), which suggests that low-T resistivity of the zero-gap semiconductor should diverge at $V_g \approx 0$. However, neither of our devices showed such behaviour. On the contrary, in the transition region between holes and electrons graphene's conductivity never falls below a well-defined value, practically independent of T between 4 K and 100 K. Figure 1c plots values of the maximum resistivity ρ_{max} found in 15 different devices at zero B, which within an experimental error of ~15% all exhibit $\rho_{max} \approx 6.5\,k\Omega$ independently of their mobility, which varies by a factor of 10. Given the quadruple degeneracy f, it is obvious to associate ρ_{max} with $h/fe^2 = 6.45\,k\Omega$, where h/e^2 is the resistance quantum. We emphasize that it is the resistivity (or conductivity) rather than the resistance (or conductance) that is quantized in graphene (that is, resistance R measured experimentally scaled in the usual manner as $R = \rho L/w$ with changing length L and width w of our devices). Thus, the effect is completely different from the conductance quantization observed previously in quantum transport experiments.

However surprising it may be, the minimum conductivity is an intrinsic property of electronic systems described by the Dirac equation[22–25]. It is due to the fact that, in the presence of disorder, localization effects in such systems are strongly suppressed and emerge only at exponentially large length scales. Assuming the absence of localization, the observed minimum conductivity can be explained qualitatively by invoking Mott's argument[26] that the mean free path l of charge carriers in a metal can never be shorter than their wavelength λ_F. Then, $\sigma = ne\mu$ can be rewritten as $\sigma = (e^2/h)k_F l$, so σ cannot be smaller than $\sim e^2/h$ for each type of carrier. This argument is known to have failed for 2D systems with a parabolic spectrum in which disorder leads to localization and eventually to insulating behaviour[22,23]. For 2D Dirac fermions, no localization is expected[22–25] and, accordingly, Mott's argument can be used. Although there is a broad theoretical consensus[15,16,23–28] that a 2D gas of Dirac fermions should exhibit a minimum conductivity of about e^2/h, this quantization was not expected to be accurate and most theories suggest a value of $\sim e^2/\pi h$, in disagreement with the experiment.

Thus, graphene exhibits electronic properties that are distinctive for a 2D gas of particles described by the Dirac equation rather than the Schrödinger equation. The work shows a possibility of studying

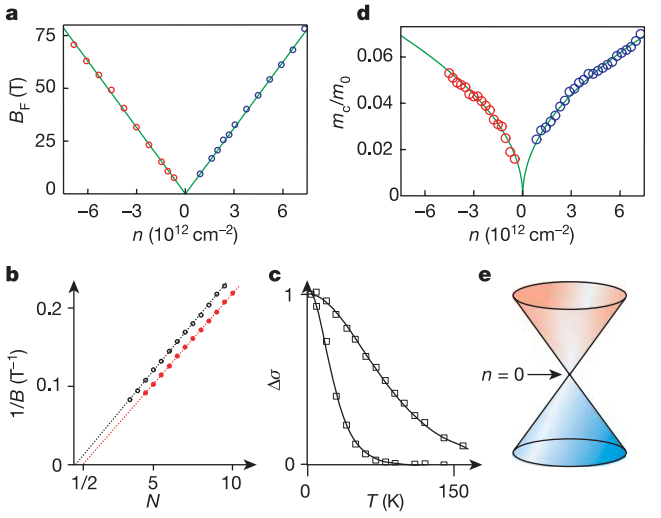

Figure 3 | Dirac fermions of graphene. **a**, Dependence of B_F on carrier concentration n (positive n corresponds to electrons; negative to holes). **b**, Examples of fan diagrams used in our analysis[7] to find B_F. N is the number associated with different minima of oscillations. The lower and upper curves are for graphene (sample of Fig. 2a) and a 5-nm-thick film of graphite with a similar value of B_F, respectively. Note that the curves extrapolate to different origins, namely to $N = 1/2$ and $N = 0$. In graphene, curves for all n extrapolate to $N = 1/2$ (compare ref. 7). This indicates a phase shift of π with respect to the conventional Landau quantization in metals. The shift is due to Berry's phase[14,20]. **c**, Examples of the behaviour of SdHO amplitude $\Delta\sigma$ (symbols) as a function of T for $m_c \approx 0.069$ and $0.023m_0$ (see the dependences showing the rapid and slower decay with increasing T, respectively); solid curves are best fits. **d**, Cyclotron mass m_c of electrons and holes as a function of their concentration. Symbols are experimental data, solid curves the best fit to theory. **e**, Electronic spectrum of graphene, as inferred experimentally and in agreement with theory. This is the spectrum of a zero-gap 2D semiconductor that describes massless Dirac fermions with c_* 1/300 the speed of light.

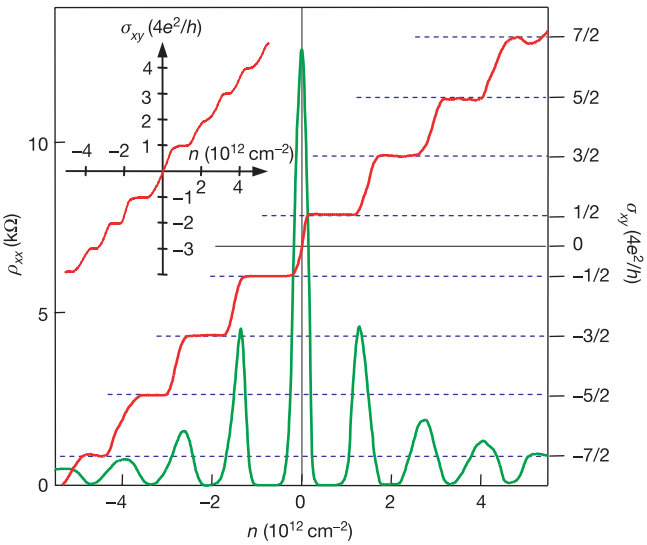

Figure 4 | QHE for massless Dirac fermions. Hall conductivity σ_{xy} and longitudinal resistivity ρ_{xx} of graphene as a function of their concentration at $B = 14$ T and $T = 4$ K. $\sigma_{xy} \equiv (4e^2/h)\nu$ is calculated from the measured dependences of $\rho_{xy}(V_g)$ and $\rho_{xx}(V_g)$ as $\sigma_{xy} = \rho_{xy}/(\rho_{xy}^2 + \rho_{xx}^2)$. The behaviour of $1/\rho_{xy}$ is similar but exhibits a discontinuity at $V_g \approx 0$, which is avoided by plotting σ_{xy}. Inset: σ_{xy} in 'two-layer graphene' where the quantization sequence is normal and occurs at integer ν. The latter shows that the half-integer QHE is exclusive to 'ideal' graphene.

phenomena of the quantum field theory in a condensed-matter experiment.

Received 14 July; accepted 12 September 2005.

1. Rose, M. E. *Relativistic Electron Theory* (Wiley, New York, 1961).
2. Berestetskii, V. B., Lifshitz, E. M. & Pitaevskii, L. P. *Relativistic Quantum Theory* (Pergamon, Oxford, 1971).
3. Lai, D. Matter in strong magnetic fields. *Rev. Mod. Phys.* **73,** 629–662 (2001).
4. Fradkin, E. *Field Theories of Condensed Matter Systems* (Westview, Oxford, 1997).
5. Volovik, G. E. *The Universe in a Helium Droplet* (Clarendon, Oxford, 2003).
6. Novoselov, K. S. *et al.* Two dimensional atomic crystals. *Proc. Natl Acad. Sci. USA* **102,** 10451–10453 (2005).
7. Novoselov, K. S. *et al.* Electric field effect in atomically thin carbon films. *Science* **306,** 666–669 (2004).
8. Zhang, Y., Small, J. P., Amori, M. E. S. & Kim, P. Electric field modulation of galvanomagnetic properties of mesoscopic graphite. *Phys. Rev. Lett.* **94,** 176803 (2005).
9. Berger, C. *et al.* Ultrathin epitaxial graphite: 2D electron gas properties and a route toward graphene-based nanoelectronics. *J. Phys. Chem. B* **108,** 19912–19916 (2004).
10. Bunch, J. S., Yaish, Y., Brink, M., Bolotin, K. & McEuen, P. L. Coulomb oscillations and Hall effect in quasi-2D graphite quantum dots. *Nano Lett.* **5,** 287–290 (2005).
11. Dresselhaus, M. S. & Dresselhaus, G. Intercalation compounds of graphite. *Adv. In Phys.* **51,** 1–186 (2002).
12. Brandt, N. B., Chudinov, S. M. & Ponomarev, Y. G. *Semimetals 1: Graphite and Its Compounds* (North-Holland, Amsterdam, 1988).
13. Vonsovsky, S. V. & Katsnelson, M. I. *Quantum Solid State Physics* (Springer, New York, 1989).
14. Gusynin, V. P. & Sharapov, S. G. Magnetic oscillations in planar systems with the Dirac-like spectrum of quasiparticle excitations. *Phys. Rev. B* **71,** 125124 (2005).
15. Gusynin, V. P. & Sharapov, S. G. Unconventional integer quantum Hall effect in grapheme. Preprint at ⟨http://xxx.lanl.gov/abs/cond-mat/0506575⟩ (2005).
16. Peres, N. M. R., Guinea, F. & Castro Neto, A. H. Electronic properties of two-dimensional carbon. Preprint at ⟨http://xxx.lanl.gov/abs/cond-mat/0506709⟩ (2005).
17. Zheng, Y. & Ando, T. Hall conductivity of a two-dimensional graphite system. *Phys. Rev. B* **65,** 245420 (2002).
18. Kaku, M. *Introduction to Superstrings* (Springer, New York, 1988).
19. Nakahara, M. *Geometry, Topology and Physics* (IOP, Bristol, 1990).
20. Mikitik, G. P. & Sharlai, Yu. V. Manifestation of Berry's phase in metal physics. *Phys. Rev. Lett.* **82,** 2147–2150 (1999).
21. Luk'yanchuk, I. A. & Kopelevich, Y. Phase analysis of quantum oscillations in graphite. *Phys. Rev. Lett.* **93,** 166402 (2004).
22. Abrahams, E., Anderson, P. W., Licciardello, D. C. & Ramakrishnan, T. V. Scaling theory of localization: Absence of quantum diffusion in two dimensions. *Phys. Rev. Lett.* **42,** 673–676 (1979).
23. Fradkin, E. Critical behaviour of disordered degenerate semiconductors. *Phys. Rev. B* **33,** 3263–3268 (1986).
24. Lee, P. A. Localized states in a d-wave superconductor. *Phys. Rev. Lett.* **71,** 1887–1890 (1993).
25. Ziegler, K. Delocalization of 2D Dirac fermions: The role of a broken symmetry. *Phys. Rev. Lett.* **80,** 3113–3116 (1998).
26. Mott, N. F. & Davis, E. A. *Electron Processes in Non-Crystalline Materials* (Clarendon, Oxford, 1979).
27. Morita, Y. & Hatsugai, Y. Near critical states of random Dirac fermions. *Phys. Rev. Lett.* **79,** 3728–3731 (1997).
28. Nersesyan, A. A., Tsvelik, A. M. & Wenger, F. Disorder effects in two-dimensional d-wave superconductors. *Phys. Rev. Lett.* **72,** 2628–2631 (1997).

Acknowledgements We thank L. Glazman, V. Falko, S. Sharapov and A. Castro Neto for discussions. K.S.N. was supported by Leverhulme Trust. S.V.M., S.V.D. and A.A.F. acknowledge support from the Russian Academy of Science and INTAS. This research was funded by the EPSRC (UK).

Author Information Reprints and permissions information is available at npg.nature.com/reprintsandpermissions. The authors declare no competing financial interests. Correspondence and requests for materials should be addressed to A.K.G. (geim@man.ac.uk) or K.S.N. (kostya@man.ac.uk).